Membrane Water Treatment, *Vol. 9, No. 1 (2018) 43-51*
DOI: https://doi.org/10.12989/mwt.2018.9.1.043

Effect of spinning parameters of polyethersulfone based hollow fiber membranes on morphological and mechanical properties

Shadia R. Tewfik, Mohamed H. Sorour, Hayam F. Shaalan and Heba A. Hani*

National Research Centre, Engineering Research Division, Chemical Engineering and Pilot Plant Department, ElBohous St. Dokki, Giza, Egypt

(Received October 25, 2016, Revised August 30, 2017, Accepted October 9, 2017)

Abstract. Hollow fiber (HF) membranes are gaining wide interest over flat membranes due to their compaction and high area to surface volume ratio. This work addresses the fabrication of HF from polysulfone (PS) and polyethersulfone (PES) using N-methylpyrrolidone (NMP) as solvent in addition to other additives to achieve desired characteristics. The semi-pilot spinning system includes jacketed vessel, four spinneret block, coagulation and washing baths in addition to dryer and winder. Different parameters affecting dry-wet spinning phase inversion process were investigated. Dope compositions of PES, NMP and polyvinyl pyrrolidone (PVP) of varying molecular weights as additive were addressed. Some critical parameters of importance were also investigated. Those include dope flow rate, air gap, coagulation & washing baths and drying temperatures. The measured dope viscosity was in the range from 1.7 to 36.5 Pa.s. Air gap distance was adjusted from 20 to 45 cm and coagulation bath temperature from 20 to 46˚C. The HF membranes were characterized by scanning electron microscope (SEM), atomic force microscope (AFM) and mechanical properties. Results indicated prevalence of finger like structure and average surface roughness from about 29 to 78.3 nm. Profile of stress strain characteristics revealed suitability of the fibers for downstream interventions for fabrication of thin film composite membrane. Different empirical correlations were formulated which enable deeper understanding of the interaction of the above mentioned variables. Data of pure water permeability (PWP) confirmed that the fabricated samples fall within the microfiltration (MF)-ultrafiltration (UF) range of membrane separation.

Keywords: hollow fiber membranes; PES; fabrication; spinning; morphology; operating parameters; permeability

1. Introduction

Polyethersulfone (PES) is considered one of the most important polymeric materials for use in water and gas membrane separation applications (Bolong *et al.* 2009; Rahimpour *et al.* 2012; Kumar *et al.* 2015). Controlling the membrane structure was a common target for improving membrane performance (Lalia *et al.* 2013) which is generally related to dope composition, spinning parameters and post treatment. (Peng *et al.* 2012, Feng *et al.* 2013, Wan and Chung 2015).

Chung *et al.* (2000), Qin and Chung (1999), Wang *et al.* (2004) studied the effect of dope flow rate of PES ultrafiltration (UF) hollow fiber (HF) membranes. It was found that higher dope flow rates in the spinneret produce UF hollow fiber membranes with smaller pore sizes and denser skin layers due to the enhanced molecular orientation leading to decrease in pore size and water permeability and increase in solute separation, tensile strength and Young's modulus. The air gap distance also plays a very important role on HF membrane performance. An increase in air gap results in a significant decrease in permeability and elimination of macrovoids, reduction of fiber dimension and also increase of fiber production rate (Chung *et al.* 1997, 2008). High viscosity of spinning dope and decreasing of water/solvent ratio as coagulation medium resulted in complete disappearance of macrovoids. In addition, reducing the coagulation bath temperature (CT) led to elimination of macrovoids as well as attaining high thermal stability (Cabasso *et al.* 1977, Dot and Hamanaka 1991, Mansoori *et al.* 2011).

Different types of polymeric additives such as polyvinyl pyrrolidone (PVP) and polyethylene glycol (PEG) were used for modification of PES membranes. These polymeric additives enhanced the surface properties of PES with an aggregation during the phase inversion process, as well as, increasing flux recovery ratio, membrane performance, pure water permeability, thermodynamic enhancement for phase separation (Han *et al.* 2002, Liu *et al.* 2003, Amirilargani *et al.* 2010, Ahmad *et al.* 2013, Zhao *et al.* 2013). However, increase of the concentration of the additives leads to increase in solution viscosity which causes kinetic hindrance against phase separation (Lee *et al.* 2003).Moreover, Ochoa *et al.* (2001) concluded that addition of different PVP molecular weight types changed mainly the surface porous structure in addition to some bulk parameters as porosity, thickness and/or tortuosity. Arahman *et al.* (2012) also studied the effect of Pluronic F127, PVP, and Tetronic 1307 on the fabrication of PES HF membranes. In addition, the inorganic additives revealed their ability to improve the structural as well as the surface properties of the PES membranes (Han *et al.* 2002). The effect of heat treatment on UF performance was explored

*Corresponding author, Ph.D.
E-mail: hi_heba2@yahoo.com

ISSN: 2005-8624 (Print), 2092-7037 (Online)

by Gholami *et al.* (2003). Their results confirmed the shrinkage of hollow fiber membranes upon heat treatment leading to a decrease in flux.

To the best of the authors' knowledge, almost all previously published work was conducted on single fiber experimental laboratory scale. This work addresses some findings extracted from a project undertaken by the National Research Centre. These findings pertain mostly to the MF and UF hollow fiber membranes which were fabricated on a four fiber semi-pilot scale spinning system which enabled integrated investigations of controlling parameters. The effects of dope composition, operating parameters, as well as, post treatment on HF membrane performance were investigated.

2. Materials and methods

2.1 Materials

Polyethersulphone (PES) flakes (Ultrason E6020 D; MW 50,000 g/L) and polysulfone (PS) pellets also supplied from (BASF, Germany) were used as the base polymers. N-methyl-2-pyrrolidone (NMP) and dimethylacetamide (DMAc) supplied from Carl-Roth and Merck, respectively were used as solvents. Poly(vinyl pyrrolidone) (PVP) of different molecular weights (30 K,90 K and 360 K) supplied from Sigma-Aldrich and Applichem were used as the pore formers. Lithium chloride (LiCl) (MW= 42.30) supplied from Alpha Chemika was used as inorganic additive. Ethanol was supplied as a lab grade solvent and reverse osmosis (RO) water was used as the bore fluid, coagulation and washing bath media.

2.2 Hollow fiber membrane fabrication

HF membranes were fabricated through a dry-wet phase inversion spinning technique by extruding a polymeric dope (PES/PS, solvents and additives) through four annular spinning nozzles with a bore fluid passing in the center of the annulus to maintain the hollow structure within the fibers. The polymer dope was created by mixing the polymer, solvent, and other ingredients in a stirred tank jacketed vessel. The dissolution takes place at 70^{o}C, 1-3 bar under nitrogen and was left overnight while stirring. The dope was then pumped using a metering pump to the spinnerets, supported on a heated spinning block with an adjustable air gap distance, where the spinning process takes place. Bore fluid (lumen side) was supplied from a pressurized vessel (0.5-2 bar) and fed to the spinnerets through a controlled flow meter. The as-spun fibers discharged from the nozzles were introduced into a water filled coagulation bath to solidify then, collected and wrapped multiple times around a speed controlled rollers and fed to two consecutive washing baths where they were rolled over other rollers and finally wound on a take-up reel winder, as shown in Fig. 1. All vessels and baths were temperature controlled. HF membranes, collected after the second washing bath, were soaked for 1 day in RO water followed by another day in 10% glycerol solution and finally left for air drying (about 25^{o}C) (samples denoted by "*a*"). Selected samples were post treated, after soaking in glycerol, using hot water at 60^{o}C for 1 h and finally left for air drying (samples denoted by "*h*"). Selected fibers were dried under controlled temperatures using a drying oven before wound on a take-up reel winder (samples denoted by "*d*"). Table 1 depicts the dope compositions and their

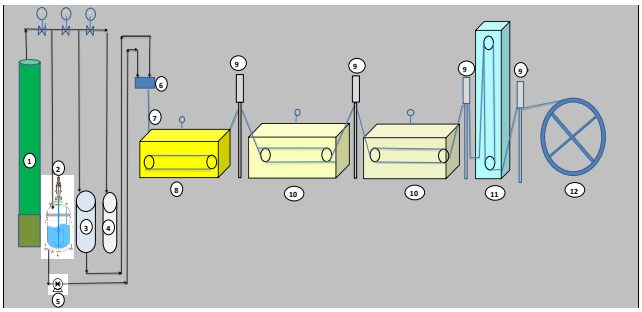

Fig. 1 Experimental set-up of PES HF membrane dry-wet spinning system, (1) Nitrogen cylinder, (2) Stirred tank jacketed vessel, (3) Bore fluid vessel, (4), Solvent vessel, (5) Dope pump, (6) Spin block, (7) Air gap, (8) Coagulation bath, (9) Take-up roll unit, (10) Washing tank, (11) Dryer and (12) Winder

Table 1 Selected dope compositions and their corresponding viscosities

Sample Code	PS (%)	PES (%)	NMP (%)	DMAC (%)	PVP 360k (%)	PVP 90k (%)	PVP 30k (%)	LiCl (%)	Ethanol (%)	Viscosity (Pa.s)
Low dope viscosities (1.74-7.9 Pa.s)										
A	0.0	17.1	77.9	0.0	0.0	0.0	5.0	0.0	0.0	1.7-1.9
B	0.0	18.2	70.8	3.5	0.0	0.0	7.0	0.5	0.0	3.3-3.7
C	0.0	22.5	66.0	0.8	0.0	0.0	7.0	0.6	3.1	7.6-7.9
Medium dope viscosities (9-18.1 Pa.s)										
D	0.0	22.5	67.3	0.0	0.0	0.0	7.0	0.6	2.6	9-9.4
E	0.0	22.5	66.9	0.0	0.0	1.0	6.0	0.6	3.0	9.8-11.2
F	0.0	17.1	70.3	0.0	5.4	3.6	3.6	0.0	0.0	10.0-10.4
G	0.0	20.0	69.0	3.5	3.0	0.0	4.0	0.5	0.0	12.3-12.7
H	0.0	18.2	70.8	3.5	3.0	2.0	2.0	0.5	0.0	15.4-18.1
High dope viscosities (24.5-36.5 Pa.s)										
I	4.4	13.2	77.4	0.0	5.0	0.0	0.0	0.0	0.0	24.5-25.0
J	0.0	18.2	74.7	0.0	3.0	2.0	2.0	0.1	0.0	28.1-32.1
K	5.7	11.5	77.8	0.0	5.0	0.0	0.0	0.0	0.0	29.0-30.6
L	8.6	8.6	77.8	0.0	5.0	0.0	0.0	0.0	0.0	31.2-32.0
M	0.0	17.5	75.5	0.0	7.0	0.0	0.0	0.0	0.0	35.5-36.5
Range of variation	4.4-8.6	8.6-22.5	66-77.8	0.0-3.5	0.0-7.0	0.0-3.6	0.0-7.0	0.0-0.6	0.0-3.1	1.7-36.5

Table 2 Ranges of the main investigated operating parameters

Investigated parameter	Value
Dope flow rate (R)	2-5 ml/min
Bore fluid flow rate (BR)	1.2-3.5 ml/min
Air gap distance(G)	20-45 cm
Coagulation bath temperature (CT)	20-46^{O}C
Washing bath temperature (WT)	20-70 ^{O}C
Drying & heating temperatures (DT) & (HT)	25-60 ^{O}C

corresponding viscosities of selected samples from more than 30 spinning experiments conducted within the scope of this work. In addition Table 2 illustrates the ranges of the different adopted operating parameters. Every sample was prepared repeatedly for 2-5 times for reproducibility.

2.3 Characterization and performance evaluation

The mechanical and morphological properties of the prepared HF membranes were characterized as elucidated below with average of five measurement values undertaken for each sample to ensure reproducibility of results.

2.3.1 Scanning electron microscopy (SEM)

The morphology of the HF membranes was studied through SEM imaging using scanning microscopes JEOL-JXA-840 A. or JEOL SEM 6000 Neoscope desktop or QUANTA FEG 250. HF samples were cut by means of a sharp razor and then they were fixed on the sample stage using carbon double-face tape. Morphological structure and HF membrane inside and outside diameter, as well as, wall thickness were evaluated.

2.3.2 Atomic force microscopy (AFM)

HF surface morphology and roughness were analyzed using 1.5 micron resolution TT-AFM workshop, equipped with a video optical microscope with up to 400X zoom. A one cm long fiber sample was fixed using a double face tape on the magnetic plate of the AFM apparatus. Vibrating scan mode was used for testing scan areas of 10µm×10µm. Roughness parameters were calculated using "Gwyddion" software. Mechanical properties of HF membranes were studied using a bench top tensile testing machine, Tinius Olsen H5kS, equipped with a 5N load cell. Testing was undertaken at 50 mm/min speed and gauge length of 100 mm.Tensile strength, elongation at break and fiber's Young's modulus were measured.

2.3.3 Pure water permeability (PWP)

Permeability tests were carried out using an apparatus for permeability measurement (PHILOS Co., Ltd) which is equipped with a high pressure pump and a feed tank connected to 3 compartments; feed, permeate and concentrate. A pre-prepared module was used containing 15-20 fibers adhered to a U shaped polyethylene hose using epoxy adhesives. PWP rate was measured at specific time and pressure using the following equation (Basile *et al.* 2010)

$$\mathrm{PWP} = \frac{\mathrm{V}}{\mathrm{A.t}} \tag{1}$$

where PWP is the pure water permeability rate ($Lm^{-2}h^{-1}$), V is the permeation volume of water (L), A is the effective membrane area (m^2) and t is the sampling time (h).

2.3.4 Membrane porosity and average pore size determination

Membrane porosity can be defined as the volume of the pores divided by the total volume of the membrane. In order to evaluate the porosity of the membrane, hollow fibers not previously treated with the glycerol solution were dried at 60 ℃ and weighed with a precision balance, then impregnated with kerosene for about 24 h and weighed again after wiping away superficial kerosene with filter paper (Bonyadi *et al.* 2009). The gravimetric method was used, which is based on measuring the weight of kerosene entrapped within the membrane pores. It is worth to mention here that the use of kerosene instead of water in porosity measurement is due to the lower surface tension which makes it more pervasive within the pores of the membrane. The overall porosity of the fiber membrane (ε) was calculated using the following formula (Feng *et al.* 2004, Simone *et al.* 2010, Drioli *et al.* 2013).

$$\varepsilon\,(\%) = \frac{\frac{(\mathrm{w1}-\mathrm{w2})}{\mathrm{Dk}}}{\frac{(\mathrm{w1}-\mathrm{w2})}{\mathrm{Dk}} + \frac{\mathrm{w2}}{\mathrm{Dpol}}} * 100 \tag{2}$$

where w1 is the weight of the wet membrane (g), w2 the weight of the dry membrane (g), Dk the density of kerosene oil (0.82 g/cm^3), Dpol is the density of polymer composite (PES and PVP) (1.336 g/cm^3). Three-five measurements were carried out and the average values were presented.

Average pore size can be determined through hydraulic permeability (Cabasso *et al.* 1977) using the Hagen-Poiseuille equation which gives the relation- ship between the pure water flux and the applied pressure across the membrane, as well as, the average porosity of the membrane, according to the following equation (Bowen *et al.* 1997).

$$\mathrm{Jw} = \frac{\mathrm{r_p^2}\,\Delta\mathrm{P}}{8\mu(\frac{\Delta\mathrm{x}}{\mathrm{A_k}})} \tag{3}$$

where Jw is the water flux based on membrane area (m/s), r_p is the average effective pore radius (m), ΔP is the trans-membrane pressure (N/m^2), μ is solution viscosity (Pa.s), Δx is the effective membrane thickness (m) and Ak is the membrane porosity.

2.3.5 Data analysis

Compiled results of the conducted experiments, regarding fibers morphology, AFM and tensile strength, were firstly analyzed for consistency and reliability. The analyzed data was correlated by applying relevant analysis methods such as multiple linear and non-linear regression and curve fitting to formulate the mathematical empirical models governing the hollow fiber preparation parameters and characteristics. Typical software used for this purpose includes Labfit (V.7.2.48), Statistica (5.0) and Microsoft Excel.

3. Results and discussion

3.1 Effect of dope composition on viscosity

The effect of blend composition, including PES, PS, PVP (k30, k90, k360), as weight % on the dope viscosity (Pa.s) was empirically correlated as presented in Eq. (4) with correlation coefficient of 0.96

$$v = 15.7 \times (PES) + 2.6 \times (PS) + 2.5 \times (PVP360) - 2.3 \times (PVP90) - 2.2 \times (PVP30) - 50.4 \tag{4}$$

where "*v*" represents the dope viscosity at viscosity ranges from 1.7 to 36.5 Pa.s. It is concluded that with increasing the polymer content, dope viscosities increase which is in

agreement with results of Chung (2008) and (Alsalhy *et al.* 2014). Fig. 2 represents the predicted versus experimental viscosity values.

3.2 Morphological findings

Morphological findings are expressed in terms of PES HF membrane thickness and dimensions of different layers within the SEM section.

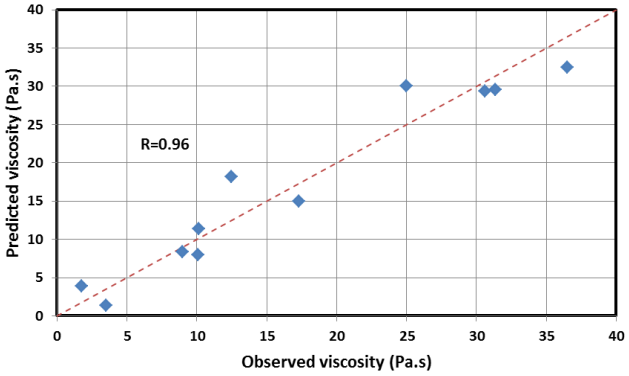

Fig. 2 Predicted viscosities vs. observed values for different PES HF membrane dopes

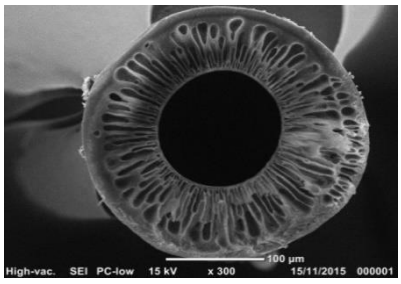

(a)

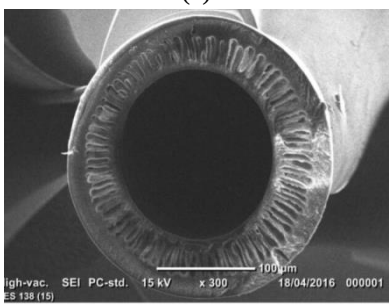

(b)

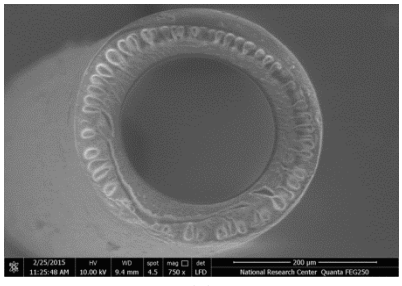

(c)

Fig. 3 SEM images of PES HF membranes at (a) low viscosity (sample B), (b) medium viscosity (sample G) and (c) high viscosity (sample J)

Table 3 Dimensions of selected PES HF membranes

Sample code	Di (µm)	Do (µm)	Thickness (µm)	Inner layer (µm)	Outer layer (µm)	Finger like layer (µm)
B	130.0	274.0	72.0	5.2	16.5	50.3
C	190.0	312.0	61.0	2.9	20.5	37.6
D	148.4	276.4	64.0	6.0	8.2	49.8
E	150.0-155.0	270.0-277.0	60.0-61.0	5.2-5.8	5.3-13.4	49.5-41.8
G	177.0	303.0	63.0	6.0	9.0	48
H	245.0-272.5	375.0-379.3	65-53.4	17.4-18	3.9-4	43.7-31.4
J	198.0	296.0	49.0	3.0	5.0	41.0

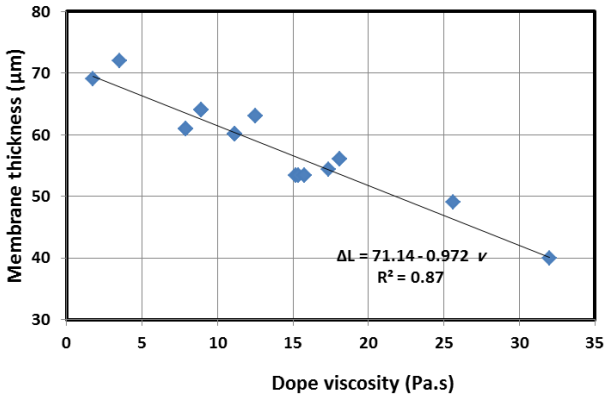

Fig. 4 Effect of dope viscosity on PES HF membrane thickness

3.2.1 Effect of viscosity on membrane thickness

Selected SEM micrographs corresponding to low, medium and high dope viscosities (samples; B, H and J, respectively) are shown in Fig. 3. SEM images show high tendency towards the formation of elongated finger-like structure at low viscosities, while as viscosities increase the spongy middle section increases significantly. All matrices present the conventional three layers structure with almost defined inner, middle and outer layer. The middle layer reflects mixed patterns of finger-like and microvoid structure. Dimensional characteristics are presented in Table 3, showing outer diameter (Do), inner diameter (Di), wall thickness (ΔL) and the three sub layers (inner layer, , finger like structure and outer layer). Samples (B) and (J) revealed the maximum and minimum thicknesses respectively.

Fig. 4 presents the effect of dope viscosity (Pa.s) on HF membrane thickness (ΔL, µm) according to the formulated empirical correlation shown on the figure. The validity ranges of viscosity and thickness were 1.74-32 Pa.s and 40-72 µm, respectively. It is clear that membrane thickness decreases with increasing dope viscosity. In this study, the decrease of viscosity is due to addition of lower molecular weight PVP (k30), decrease in polymer content and ethanol addition. It should be noted that Alsalhy *et al.* (2014) indicated increasing membrane thickness with increasing dope viscosity due to the addition of PEG at constant PES concentration while, Mustaffar *et al.* (2005) mentioned that the polymer concentration in dope solution did not affect directly the overall cross section structure of the HF membrane. Such apparent different results should acknowledge different sample history, composition,

spinning parameters and post spinning interventions.

3.2.2 *Effect of air gap distance on membrane thickness*

Air gap distance was found to affect the HF membrane thickness as shown in Fig. 5. It is observed that the HF membrane thickness decreases linearly with increasing the value of air gap distance investigated which is in agreement with the findings of Chung *et al.* (1997) and Khulbe el al. (2003) for PES/polyimide HF membranes. This denotes the effect of gravitational forces and molecular orientation. The depicted derived empirical correlation manifests the pre-mentioned trend as presented in Fig. 5 with correlation coefficient of 0.86. The validity ranges for air gap and membrane thickness are 20-45 cm and 29-70.5 µm, respectively. The difference in thickness for typical samples at different air gap distances (45 cm and 30 cm) is clearly demonstrated in the SEM images shown in Fig. 6.

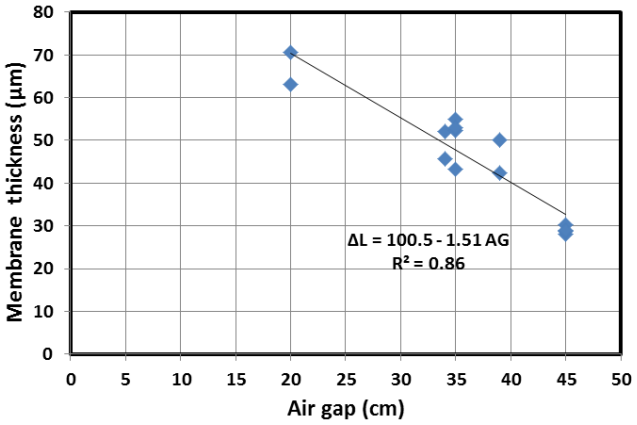

Fig. 5 Effect of air gap on PES HF membrane thickness

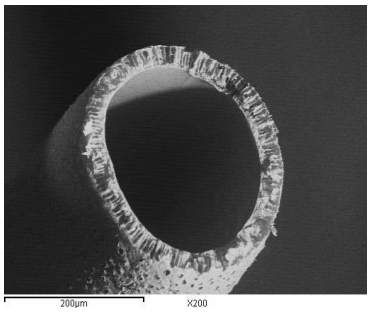

(a)

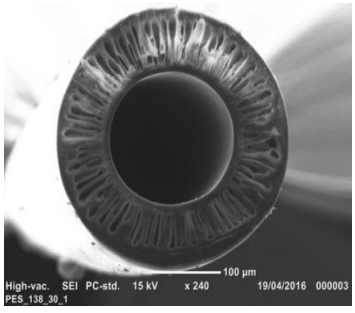

(b)

Fig. 6 SEM images of PES HF membranes at air gap distance (a) 45 cm and (b) 30 cm

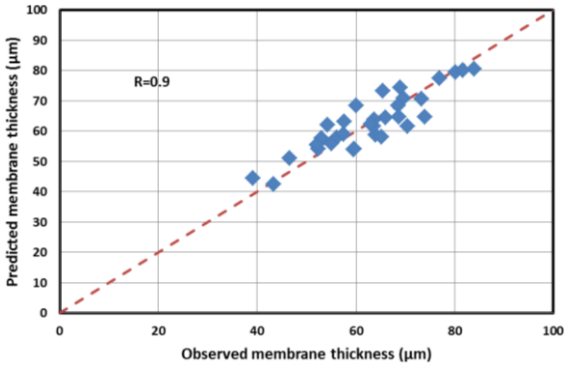

Fig. 7 Predicted membrane thickness vs. observed values from Eq. (5)

3.2.3 *Effect of processing parameters on membranes thickness*

An empirical correlation was formulated to present the effect of the investigated processing parameters including; dope viscosity (v), dope flow rate (R), air gap (G), coagulation bath temperature (CT), washing bath temperature (WT) and drying temperature (DT) on the HF membrane thickness as shown in below in Eq. (5).

$$\Delta L\ (\mu m) = 35.7 - 26.5 \times v_n + 38.2 \times R_n + 5 \times G_n + 6 \times CT_n - 1.6 \times \frac{70}{WT_n} + 7 \times \frac{60}{DT_n} \quad (5)$$

The data (denoted by (n)) is normalized to the maximum observed value of each parameter. The correlation coefficient of this equation is 0.9. Fig. 7 represents the predicted versus experimental PES HF membrane thickness values.

3.3 AFM findings

The effect of dope viscosity (1.74-18.13 Pa.s) on observed average surface roughness (Ra) (29-78.3 nm) is shown in Fig. 8. The HF membrane roughness increases linearly with increasing dope viscosity. Typical roughness images for samples (B, G and H) are shown in Fig. 9. Surface roughness affects positively and negatively membrane performance. For low pressure applications, the presence of roughness increases fouling potential; thus, low roughness membranes are preferred. If the membranes will undergo subsequent coating or surface treatment, a certain degree of surface roughness maybe required to increase attachment of the polyamide coat layer to the membrane support.

3.4 Mechanical characteristics

Our endeavors were limited to investigating tensile strength at break, strain at break and young's modulus. The mean and standard deviation of observed tensile strength, break strain and Young's Modulus for wet and dry HF membrane samples are presented in Table 4. These values are comparable or even exceed the findings of Alsalhy *et al.* (2014), Wan *et al.* (2017) and Zhang *et al.* (2014). The decrease of Young's modulus from 407 MPa to 170 MPa due to increasing the dope viscosity from 3.5-18.125 Pa.s was empirically correlated, as shown in Fig. 10.

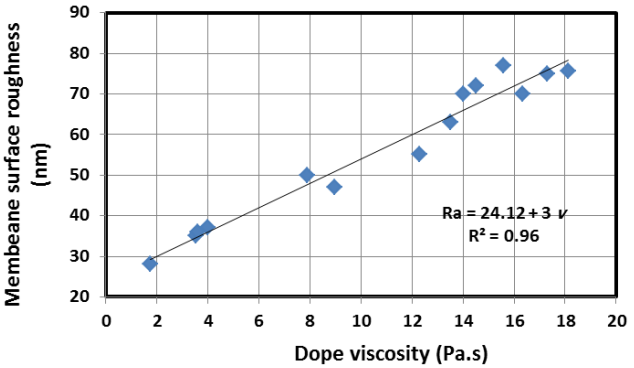

Fig. 8 Effect of surface roughness at different dope viscosities

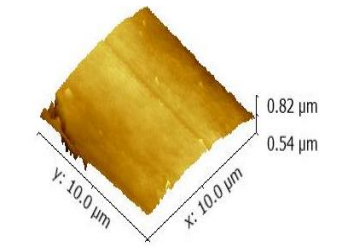

(a)

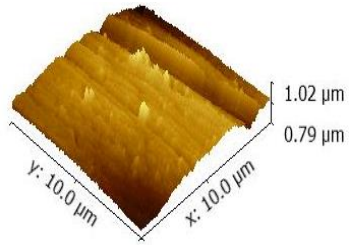

(b)

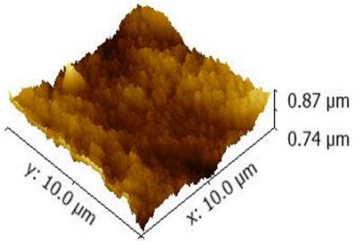

(c)

Fig. 9 Surface roughness images of membranes of selected samples (a) B, (b) G and (c) H

3.5 Pure water permeability (PWP)

The effect of PWP for samples (B and H) at low and medium viscosity ranges, respectively within a pressure range (1-5 bar) is shown in Fig. 11**.** Sample H was tested after post treatment using air drying (H_a), oven drying at 40°C (H_d) and heat treatment in hot water at 60°C (H_h). General trend reveals lower permeabilities for dried and heated samples than the raw sample. The PWP is reduced from 3000 L/m^2.h (sample (H_a)) to 2100 L/m^2.h (sample (H_d)) at 5 bar while, further heating using hot water (sample (H_h)) at 60˚C reduces PWP dramatically to 1200 L/m^2.h. This is believed to be a direct consequence of pore size shrinkage. The results are comparable with the trend

Table 4 Mechanical properties for wet and dry samples

Samples	Tensile Strength (MPa)	Break strain (%)	Young's modulus (MPa)
Wet	11.3 (0.96)	47.96 (3.03)	312.6 (35.0)
Dry	11.5 (1.10)	39.3 (3.15)	314.6 (40.5)

The values in the brackets were standard deviation

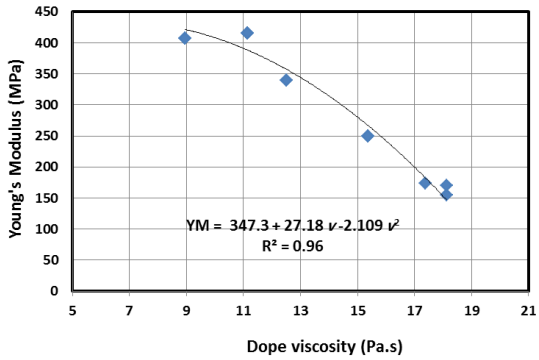

Fig. 10 Effect of dope viscosities on PES HF membrane Young's modulus

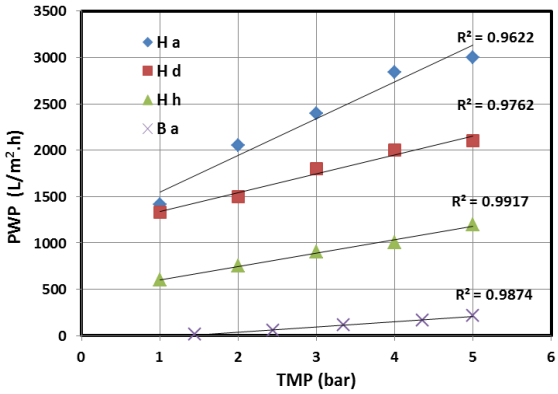

Fig. 11 HF PES membrane water permeability of, a) air dried, d) oven dried and h) heated samples

reported by Gholami *et al.* (2003), Wang *et al.* (2004) and Feng *et al.* (2013). Lower fluxes (215 at 5 bar) are observed for sample (B_a) prepared with the same PES concentration used for sample (H) but using lower molecular weight PVP (k30) which insures uniform dispersion of the hydrophilic polymer with lower pore size. Data for PWP confirmed that the fabricated HF membranes fall within MF-UF range (Carvalho *et al.* (2010), Alsalhy *et al.* (2014). Generally, these data suggest further investigations for the effect of heat treatment using conventional and microwave drying on membrane structure and performance.

3.6 Membrane porosity

Average membrane porosity for sample (H_d) was determined by gravimetric method using kerosene, as illustrated in section 2.3.4. The average porosity of PES HF membrane was found to be 72.8%. This value is comparable with those of PES HF membranes studied by Alsalhy *et al.* (2014). The corresponding average pore sizes at studied TMP 1-5 bar, estimated from Hagen-Poiseuille equation (3), varied from 28-50 nm which corresponds to

UF range. These results are in good agreement with Cabasso *et al.* (1977).

4. Conclusions

Different parameters affecting dry-wet spinning phase inversion process were investigated. Dope compositions of PES, NMP and varying molecular weight PVP were addressed. Some critical parameters of importance were investigated. Those include dope viscosity, dope flow rate, air gap, washing and coagulation baths and drying temperatures. SEM, AFM and mechanical characterization methods were employed to characterize morphological, roughness and some mechanical properties. Different empirical correlations were formulated including membrane thickness to various processing parameters through a non-linear relationship, dope viscosity in the range from 1.7 to 36.5 Pa.s to surface roughness and Young's modulus. These relationships enable deeper understanding of the interaction of the above mentioned variables. Further, the mean tensile strength and Young's Modulus exceeded 11 and 212 MPa for both wet and dry prepared fibers which reflect good mechanical strength. Data of pure water permeability confirms that the fabricated samples fall within 100 and 3500 L/m^2.h at TMP 1 to 5 bar which is the MF-UF range of membrane separation. Investigations are currently underway to further explore the effect of post-treatment on membrane characteristics. Emphasis is placed upon dynamics of demixing, microwave drying and coating by interfacial polymerization.

Acknowledgements

This work was undertaken through a project entitled "Technological and Engineering Development for Production of Desalination Hollow Fiber Membranes" undertaken by the National Research Centre, Egypt with financial support by Islamic Development Bank, Kuwait Development Bank and Academy of Scientific Research through the Ministry of International Cooperation.

References

Ahmad, A.L., Abdulkarim, A.A., Ooi, B.S. and Ismail, S. (2013), "Review recent development in additives modifications of polyethersulfone membrane for flux enhancement", *Chem. Eng. J.*, **223**, 246-267.

Alsalhy, Q.F., Salih, H.A., Simone, S., Zablouk, M., Drioli, E. and Figoli, A. (2014), "Polyethersulfone (PES) hollow-fiber membranes prepared from various spinning parameters", *Desalination*, **345**, 21-35.

Amirilargani, M., Sadrzadeh, M. and Mohammadi, T. (2010), "Synthesis and characterization of polyethersulfone membranes", *J. Polym. Res.*, **17**(3), 363-377.

Arahman, N., Arifin, B., Mulyati, S., Ohmukai, Y. and Matsuyama, H. (2012), "Structure change of polyethersulfone hollow fiber membrane modified with pluronic F127, polyvinylpyrrolidone, and tetronic 1307", *Mater. Sci. Appl.*, **3**(2), 72-77.

Basile, A. and Gallucci, F. (2010), *Membranes for Membrane Reactors: Preparation, Optimization and Selection*, John Wiley & Sons.

Bolong, N., Ismail, A.F., Salim, M.R., Rana, D. and Matsuura, T. (2009), "Development and characterization of novel charged surface modification macromolecule to polyethersulfone hollow fiber membrane with polyvinylpyrrolidone and water", *J. Membr. Sci.*, **331**(1), 40-49.

Bonyadi, S. and Chung, T. (2009), "Highly porous and macrovoid-free PVDF hollow fibre membranes for membrane distillation by a solvent-dope solution co-extrusion approach" *J. Membr. Sci.*, **331**(1), 66-74.

Bowen, W.R., Mohammad, A.W. and Hilail, N. (1997), "Characterisation of nanofiltration membranes for predictive purposes-use of salts, uncharged solutes and atomic force microscopy", *J. Membr. Sci.*, **126**(1), 91-105.

Cabasso, I., Klein, E. and Smith, J. (1977), "Polysulfone hollow fibers. II. Morphology", *J. Appl. Polym. Sci.*, **21**(1), 165-180.

Carvalho, L.M.J. and Silva, C.A.B. (2010), "Clarification of pineapple juice by microfiltration", *Food Sci. Technol.*, **30**(3), 823-832.

Chung, T.S. and Hu, X. (1997), "The effect of air-gap distance on the morphology and thermal properties of polyethersulfone hollow fibers", *J. Appl. Polym. Sci.*, **66**(6), 1067-1077.

Chung, T.S., Qin, J.J. and Gua, J. (2000), "Effect of shear rate within the spinneret on morphology, separation performance and mechanical properties of ultrafiltration polyethersulfone hollow fiber membranes", *Chem. Eng. Sci.*, **55**(6), 1077-1091.

Chung, T.S.N. (2008), *Fabrication of Hollow-Fiber Membranes by Phase Inversion*, in *Advanced Membrane Technology and Applications*, John Wiley& Sons, Inc., Hoboken, New Jersey, U.S.A.

Dot, S., and Hamanaka, K. (1991), "Pore size control technique in the spinning of polysulfone hollow fiber ultrafiltration membranes", *Desalination*, **80**(2), 167-180.

Drioli E., Ali, A., Simone, S., Macedonio, F., AL-Jlil, S.A., Al Shabonah, F.S., Al-Romaih, H.S., Al-Harbi, O., Figoli, A. and Criscuoli, A. (2013), "Novel PVDF hollow fiber membranes for vacuum and direct contact membrane distillation applications", *Sep. Purif. Technol.*, **115**, 27-38.

Feng, C.S., Shi, B., Li, G. and Wu, Y. (2004), "Preparation and properties of microporous membrane from poly(vinylidene fluoride cotetrafluoroethylene) (F2.4) for membrane distillation", *J. Membr. Sci.*, **237**(1), 15-24.

Feng, C.Y., Khulbe, K.C., Matsuura, T. and Ismail, A.F. (2013), "Recent progresses in polymeric hollow fiber membrane preparation, characterization and applications", *Sep. Purif. Technol.*, **111,** 43-71.

Gholami, M., Nasseri, S., Feng, C.Y., Matsuura, T. and Khulbe, K.C. (2003), "The effect of heat treatment on the ultrafiltration performance of polyethersulfone (PES) hollow-fiber membranes", *Desalination*, **155** (3), 293-301.

Han, M.J. and Nam, S.T. (2002), "Thermodynamic and rheological variation in polysulfone solution by PVP and its effect in the preparation of phase inversion membrane", *J. Membr. Sci.*, **202**(1), 55-61.

Khulbe, K.C., Feng, C., Matsuura, T., Kapantaidakis, G.C., Wessling, M. and Koops, G.H. (2003), "Characterization of polyethersulfone-polyimide hollow fiber membranes by atomic force microscopyand contact angle goniometry", *J. Membr. Sci.*, **226**(1), 63-73.

Kumar, R.S., Arthanareeswaran, G., Paul, D. and Kweon, J.H. (2015), "Modification methods of polyethersulfone membranes for minimizing fouling-Review", *Membr. Water Treat.*, **6**(4), 323-337.

Lalia, B.S., Kochkodan, V., Hashaikeh, R. and Hilal, N. (2013), "A review on membrane fabrication: Structure, properties and

performance relationship", *Desalination*, **326**, 77-95.
Lee, K.W., Seo, B.K., Nam, S.T. and Han, M.J. (2003), "Trade-off between thermodynamic enhancement and kinetic hindrance during phase inversion in the preparation of polysulfone membranes", *Desalination*, **159**(3), 289-296.
Liu, Y., Koops, G.H. and Strathmann, H. (2003), "Characterization of morphology controlled polyethersulfone hollow fiber membranes by the addition of polyethylene glycol to the dope and bore fluid solution", *J. Membr. Sci*., **223**(1), 187-199.
Mansoori, S.A.A., Pakizeh, M. and Chenar, M.P. (2011), "Effect of synthesis parameters on structural characteristics of polysulfone membrane and its gas separation properties", *J. Membr. Sci. Technol*., **1**, 1-7.
Mustaffar, M.I., Ismail, A.F. and Illias R.M. (2005), "Study on the effect of polymer concentration on hollow fiber ultrafiltration membrane", *Proceedings of the Regional Conference on Engineering Education*, Johor, Malaysia, December.
Ochoa, N.A., Prádanos, P. Palacio, L., Pagliero, C., Marchese, J. and Hernández, A. (2001), "Pore size distributions based on AFM imaging and retention of multi-disperse polymer solutes: Characterization of polyethersulfone UF membranes with dopes containing different PVP", *J. Membr. Sci*., **187**(1), 227-237.
Peng, N., Widjojo, N., Sukitpaneenit, P., Teoh, M.M., Lipscomb, G.G., Chung, T.S. and Lai, J.Y. (2012), "Evolution of polymeric hollow fibers as sustainable technologies: Past, present and future", *Prog. Polym. Sci*., **37**(10), 1401-1424.
Qin, J. and Chung, T.S. (1999), "Effect of dope flow rate on the morphology, separation performance, thermal and mechanical properties of ultrafiltration hollow fiber membranes", *J. Membr. Sci*., **157**(1), 35-51.
Rahimpour, A., Jahanshahi, M., Khalili, S., Mollahosseini, A., Zirepour, A. and Rajaeian, B. (2012), "Novel functionalized carbon nanotubes for improving the surface properties and performance of polyethersulfone (PES) membrane", *Desalination*, **286**, 99-107.
Simone S., Figoli, A., Criscuoli, A., Carnevale, M.C., Rosselli, A. and Drioli, E. (2010), "Preparation of hollow fibre membranes from PVDF/PVP blends and their application in VMD", *J. Membr. Sci*., **364**(1), 219-232.
Wan, C.F. and Chung, T.S. (2015), "Osmotic power generation by pressure retarded osmosis using seawater brine as the draw solution and wastewater brine as the feed", *J. Membr. Sci*., **479**, 148-158.
Wan, C.F., Li, B., Yang, T. and Chung, T.S. (2017), "Design and fabrication of inner-selective thin film composite (TFC) hollow fiber modules for pressure retarded osmosis (PRO)", *Sep. Purif. Technol*., **172**, 32-42.
Wang, K. Y., Matsuura, T., Chung, T.S. and Guo, W.F. (2004), "The effects of flow angle and shear rate within the spinneret on the separation performance of poly (ethersulfone) (PES) ultrafiltration hollow fiber membranes", *J. Membr. Sci*., **240**(1), 67-79.
Zhang, S., Sukitpaneenit, P. and Chung, T.S. (2014), "Design of robust hollow fiber membranes with high power density for osmotic energy production", *J. Chem. Eng*., **241**, 457-465.
Zhao, C., Xue, J., Ran, F. and Sun, S. (2013), "Modification of polyethersulfone membranes-A review of methods", *Prog. Mater. Sci*., **58**(1), 76-150.

ED

Appendix

A	Effective membrane area (m^2)
Ak	Average membrane porosity.
CT	Coagulation bath temperature (^oC)
Di	Inside membrane diameter (µm)
DMAc	Dimethylacetamide
Dk	Density of kerosene (g/cm^3)
Dpol	Density of polymer composite (g/cm^3)
Do	Outside membrane diameter (µm)
DT	Drying temperature (^oC)
G	Air gap (cm),
HF	Hollow Fiber
HT	Heating temperature (^oC)
Jw	Water flux based on membrane area (m/s)
MF	Microfiltration
NMP	N-methyl-2-pyrrolidone
PEG	Polyethylene glycol
PES	Polyethersulphone
PVP	Polyvinylpyrrolidone
PWP	Pure Water Permeability ($L/(m^2 \cdot h)$)
R	Dope flow rate (ml/min),
r_p	Average effective pore radius (m),
T	Sampling time (h)
UF	Ultrafiltration
V	Permeation volume of water (L)
w1	Weight of the wet membrane (g)
w2	Weight of the dry membrane (g)
WT	Washing bath temperature (^oC)
a	Air dried sample
h	Heat treated sample
d	Oven dried sample
µ	Solution viscosity (Pa.s)
v	Dope viscosity (Pa.s)
ε	Average membrane porosity (%)
ΔL	Membrane thickness (µm)
ΔP	Trans-membrane pressure (N/m^2)
Δx	Membrane thickness (m)